

Successful Identification of Cardiac Troponin Calcium Sensitizers Using a Combination of Virtual Screening and ROC Analysis of Known Troponin C Binders

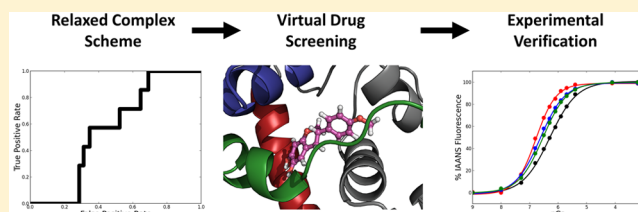
Melanie L. Aprahamian,[†] Svetlana B. Tikunova,[‡] Morgan V. Price,[‡] Andres F. Cuesta,[‡] Jonathan P. Davis,[‡] and Steffen Lindert^{*,†}

[†]Department of Chemistry and Biochemistry, Ohio State University, Columbus, Ohio 43210, United States

[‡]Davis Heart and Lung Research Institute and Department of Physiology and Cell Biology, Ohio State University, Columbus, Ohio 43210, United States

S Supporting Information

ABSTRACT: Calcium-dependent cardiac muscle contraction is regulated by the protein complex troponin. Calcium binds to the N-terminal domain of troponin C (cNTnC) which initiates the process of contraction. Heart failure is a consequence of a disruption of this process. With the prevalence of this condition, a strong need exists to find novel compounds to increase the calcium sensitivity of cNTnC. Desirable are small chemical molecules that bind to the interface between cTnC and the cTnI switch peptide and exhibit calcium sensitizing properties by possibly stabilizing cTnC in an open conformation. To identify novel drug candidates, we employed a structure-based drug discovery protocol that incorporated the use of a relaxed complex scheme (RCS). In preparation for the virtual screening, cNTnC conformations were identified based on their ability to correctly predict known cNTnC binders using a receiver operating characteristics analysis. Following a virtual screen of the National Cancer Institute's Developmental Therapeutic Program database, a small number of molecules were experimentally tested using stopped-flow kinetics and steady-state fluorescence titrations. We identified two novel compounds, 3-(4-methoxyphenyl)-6,7-chromanediol (NSC600285) and 3-(4-methylphenyl)-7,8-chromanediol (NSC611817), that show increased calcium sensitivity of cTnC in the presence of the regulatory domain of cTnI. The effects of NSC600285 and NSC611817 on the calcium dissociation rate was stronger than that of the known calcium sensitizer bepridil. Thus, we identified a 3-phenylchromane group as a possible key pharmacophore in the sensitization of cardiac muscle contraction. Building on this finding is of interest to researchers working on development of drugs for calcium sensitization.



INTRODUCTION

Heart failure, a condition that affects nearly 5.7 million Americans each year, occurs when the cardiac muscle is unable to pump enough oxygenated blood to the rest of the body resulting in improper function. Contraction of the cardiac muscle is made possible by the intricate interaction between several proteins.¹ Malfunction of any of these proteins can lead to heart failure, typically due to hindered contraction. The key players in cardiac muscle contraction are the thick (made up of myosin) and the thin (containing actin, tropomyosin, and troponin) filaments.² Binding of myosin heads to the thin filament, and subsequent conformational changes in myosin create mechanical force and ultimately contraction. This process occurs in a Ca²⁺ dependent manner.^{3,4} Cardiac troponin (cTn) is a key regulatory protein nexus in this contraction process. The cardiac troponin complex consists of three subunits: troponin C (cTnC), the subunit that binds calcium; troponin I (cTnI), the inhibitory subunit; and troponin T (cTnT), the subunit that secures the troponin complex to tropomyosin-actin.^{4–7} The structures of all three subunits of cTn are shown in Figure 1. When Ca²⁺ binds to the

N-terminal regulatory domain of cardiac troponin C, cNTnC (cTnC residues 1–89), the exposure of a hydrophobic patch between the helices A and B, as shown in Figure 2, becomes more likely.⁸ This pocket can bind the cTnI_{144–163} switch peptide and thereby initiate contraction.^{5,9,10}

A potential treatment for heart failure is the development of cardiac inotropes—agents that affect muscle contraction. Many different inotropes have been discovered over the years that affect the molecular landscape involved in cardiac contraction. These compounds include cardiac glycosides, β -adrenoceptor agonists, and phosphodiesterase inhibitor.^{11–13} The mechanisms of these compounds all act to increase calcium levels within cardiomyocytes (i.e., calcium mobilizers).¹⁴ However, adverse effects such as myocardial ischemia (decreased blood flow to the heart) and arrhythmias (abnormal heart beat)¹³ directly result from the use of these inotropes. Another mechanism by which inotropes have been found to aid against heart failure is through calcium sensitization. Such calcium

Received: September 7, 2017

Published: November 16, 2017

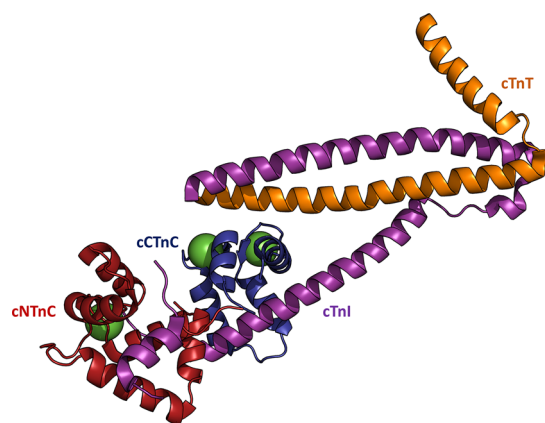


Figure 1. Structure of cardiac troponin [PDB 1JIE⁸⁹]. Each subunit is represented in a different color (cNTnC in red, cTnC in blue, cTnI in purple, and cTnT in orange). The bound Ca^{2+} ions are represented as green spheres.

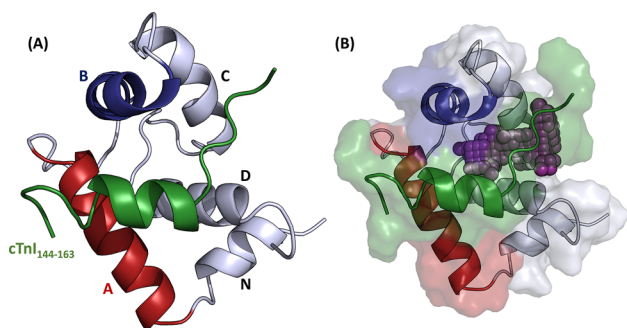


Figure 2. N-terminal regulatory domain of troponin C (residues 1–89) complexed with the cTnI switch peptide (residues 144–163) [2LIR]. (A) Location of cTnI_{144–163} between helices A and B of cNTnC. (B) Hydrophobic pocket between helices A and B represented as purple spheres.

sensitizing compounds may affect cNTnC's calcium affinity, while ideally not altering the intracellular Ca^{2+} concentrations. This mechanism has the potential to avoid many of the adverse side effects associated with other drugs.¹⁵

The most widely studied calcium sensitizer is levosimendan.^{16–18} Levosimendan is a positive inotropic compound that binds to cTnC and acts to prolong the Ca^{2+} bound conformation of isolated cTnC.¹⁷ Despite knowing the effects of levosimendan on cardiomyocytes, the exact binding mechanism on cTnC is still under debate.^{16,17,19} Currently, no experimental structure has been obtained for levosimendan bound to cTnC, but a model has been built showing levosimendan bound to the hydrophobic pocket of cNTnC.²⁰ Levosimendan has been through several clinical trials but has yet to be approved in either the US or Canada.²¹ It is currently available in Europe and Japan under the trade name Simdax. Pimobendan is another positive inotrope with vasodilating effects.²² It has undergone clinical trials and is currently used in veterinary medicine as a treatment for congestive heart failure in canines.^{23–25} Another calcium sensitizing compound more recently discovered is NSC147866 which has been shown to bind to both cNTnC and the cNTnC–cTnI_{147–163} complex.^{10,26} Other compounds reported to bind to the hydrophobic pocket of cNTnC are bepridil,^{10,22,27} W7,^{10,28} DFBP-O,^{10,26,29} and trifluoperazine.^{22,27,30} The chemical structures of these compounds are shown in Figure 3.

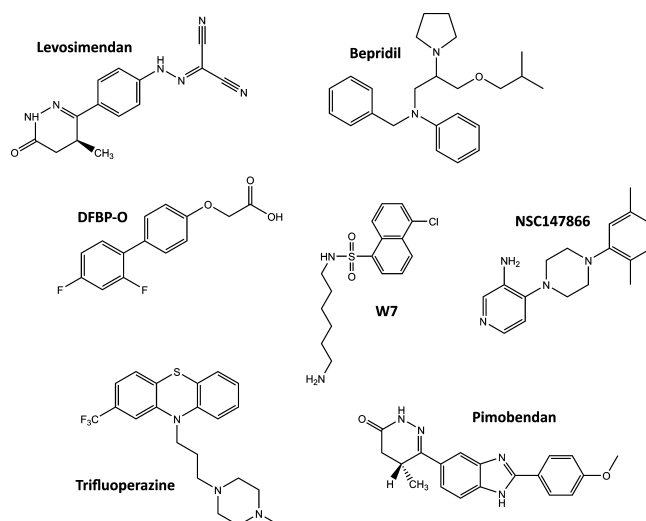


Figure 3. Chemical structures of several calcium-sensitizing compounds that bind to cNTnC.

Structure-based computer-aided drug discovery methods can facilitate the search for novel small molecules binding to the hydrophobic pocket of cNTnC.³¹ Molecular dynamics simulations have shown that calcium-bound cNTnC exhibits significant structural flexibility, allowing it to transiently open the hydrophobic pocket between helices A and B.^{8,32,33} Therefore, methods explicitly accounting for receptor flexibility in computer-aided drug design³⁴ should be used for cNTnC structure-based drug discovery. The relaxed complex scheme (RCS) is a virtual screening method that accounts for both ligand and protein receptor flexibility.^{35–37} Traditionally, computational docking calculations utilize static receptor structures and allow for the ligand to be flexible. The most common applications of the RCS method use multiple receptor structures obtained from a molecular dynamics (MD) simulations starting from a crystal or NMR structure that contains a docked ligand. Variations of the RCS have been successfully used in several virtual drug discovery studies,^{38–46} including in the identification of a low affinity calcium-sensitizing agent.²⁶

The RCS method used in this study was performed in conjunction with a structure-based virtual screening of a large database of compounds, a widely used screening technique.^{26,47} An alternative to a structure-based virtual screening method for identifying potential active ligands is to use a ligand-based screening method.^{48,49} This method does not depend upon knowledge of the receptor structure and relies solely upon the chemical structure and composition of the known active ligands, and machine learning techniques are then used to discover patterns in known actives. This is followed by screening large compound databases for compounds that have some degree of similarity to the active ligands. However, for cTnC, the number of known active ligands is relatively small and thus excludes ligand-based screening approaches.

To identify novel compounds that demonstrate stronger calcium sensitization in cNTnC, we have employed the relaxed complex scheme to determine likely candidate compounds and experimentally verified them using a combination of stopped-flow kinetics and calcium fluorescence titrations. However, cNTnC conformations for the RCS were not selected based on purely geometric considerations (in a previous study, cNTnC conformations were picked based on an RMSD clustering

Table 1. Table of Three Ligand Preparation Method Parameters Tested on the 1000 Decoy and 7 Active Compounds

LigPrep Method	Ionization	Stereoisomers	Force Field	Generate Tautomers?	Generate at Most per Ligand	Prepared Ligands Generated
1	Generate possible states at target pH 7.4, EPIK	Determine chiralities from 3D structures	OPLS_2005	Yes	5	1105
2	Generate possible states at target pH 7.4, Ionizer	Determine chiralities from 3D structures	OPLS_2005	Yes	5	1392
3	Generate possible states at target pH 7.4, Ionizer	Generate all combinations	OPLS_2005	Yes	5	1946

analysis²⁶). The goal of this study was to identify cNTnC-CtNtI₁₄₄₋₁₆₃ conformations and a ligand preparation method that are highly predictive of Ca²⁺ sensitizer binding. This was accomplished by utilizing knowledge of a set of known cNTnC binders in combination with a receiver operator characteristic analysis. Those conformations were subsequently used in RCS-type virtual screening. We experimentally tested the top compounds from the screen using stopped-flow kinetics and steady-state fluorescence Ca²⁺ titrations. This resulted in the identification of two new compounds, NSC600825 (3-(4-methoxyphenyl)-6,7-chromanediol) and NSC611817 (3-(4-methylphenyl)-7,8-chromanediol), which show promise as Ca²⁺ sensitizers of cNTnC.

METHODS AND MATERIALS

Selection of 35 Representative cNTnC Conformations as a Test Set.

A test set of cNTnC and cNTnC-cTnI₁₄₄₋₁₆₃ conformations was obtained from a combination of structures from the protein data bank and a 100 ns molecular dynamics (MD) simulation of DFBP-O bound cNTnC-Ca²⁺-cTnI₁₄₄₋₁₆₃.²⁶ A total of 35 different cNTnC and cNTnC-cTnI₁₄₄₋₁₆₃ conformations were chosen as the test set. Of the 35 conformations, five conformations were taken from crystal and NMR structures deposited in the protein data bank that had a known active compound bound to the hydrophobic pocket. Three of these conformations were cNTnC-cTnI₁₄₄₋₁₆₃ conformations: 1XLF [contained bepridil],⁵⁰ 2KRD [contained w7],⁵¹ and 2L1R [contained DFBP-O].²⁹ The other two were cNTnC conformations: 1WRK [contained trifluoperazine]²⁸ and 2KFX [contained w7].⁵²

The remaining 30 conformations were extracted from a 100 ns MD simulation of a calcium sensitizer (DFBP-O) bound complex of cNTnC-Ca²⁺-cTnI₁₄₄₋₁₆₃, the details of which have been previously reported.²⁶ This simulation of a DFBP-O bound complex of cNTnC-Ca²⁺-cTnI₁₄₄₋₁₆₃ was chosen as it corresponds to the method used to identify NSC147866. The 100 ns simulation demonstrated clear convergence after 20 ns indicating that any structures selected from the trajectory are valid representations of the conformational ensemble of the protein (Supporting Information, Figure S1). From this MD simulation, 15 frames (corresponding to snapshots of the simulation at various points in time) were chosen as potential representative conformations based upon an RMSD cluster analysis, which was detailed in a previous paper.²⁶ In addition, pocket-volume calculations were performed to determine additional cNTnC conformations that exhibit large hydrophobic pockets. These calculations were done using POVME.⁵³ Pocket volumes were calculated for each trajectory every 20 ps, resulting in 5000 pocket-volume measurements. The analysis was performed on the MD trajectory frames with the DFBP-O ligand coordinates removed. The coordinates for the inclusion sphere were extracted from coordinates of the docked ligand in the initial frame of the trajectory. A single inclusion sphere was

used with a radius of 10 Å. For the conformations for the test set, 15 frames were chosen that had large pocket volumes (>195 Å³) and were distributed evenly throughout the entire 100 ns trajectory.

Prior to performing any docking calculations, each of the 35 receptor protein conformations were prepared using Schrödinger's Protein Preparation Wizard,⁵⁴ resulting in conformations that were optimized and hydrogenated and therefore suitable for use with Glide XP.⁵⁵⁻⁵⁷ The bound ligands, Ca²⁺ ions, and any water molecules were removed from the conformations. The preparation process was done by first deleting all water molecules. The conformations were then repaired by filling in any missing residues. Lastly, a restrained minimization using the OPLS_2005 force field⁵⁸ was run on the protein structure with a restraint RMSD tolerance of 0.30 Å.

Finally, a receptor grid was created for each of the 35 conformations. Glide utilizes a grid-based docking algorithm that requires an active site identification.⁵⁶ This grid defines a 3D box that encompasses the coordinate space that is used for positioning the ligand. For each of the 35 receptors, a box center and dimensions were defined in this grid generation process. For receptors #1-5, the box centers were taken as the central coordinates of the experimental ligand, respectively. For receptors #6-35, the center coordinates of the box corresponded to the central coordinates of the bound DFBP-O in the initial frame of the trajectory. The dimensions of the box were chosen as 15 Å in each dimension.

Active and Decoy Ligand Test Set. A test set of 1007 ligands was compiled and contained both ligands known to be active in the hydrophobic pocket of cNTnC and ligands assumed to be inactive (referred to as decoys). A total of 7 ligands were chosen as actives. These ligands are shown in Figure 3. The known active ligand coordinates were taken from either a crystal/NMR structure (bepridil [1LXF], W7 [2KRD], DFBP-O [2L1R], trifluoperazine [1WRK]) or manually built in Maestro⁵⁹ using the known chemical structure (pimobendan, levosimendan, NSC147866). The "1K Drug-Like Ligand Decoy" set^{55,56} was chosen as the decoy set. It contained 1000 ligands with an average molecular mass of 360 Da, comparable to the average size of the known active ligands (325 Da). In terms of volume, the decoy set selected contains molecules with molecular volumes that are also comparable to the active ligand set (Supporting Information, Figure S2).

Selection of Highly Predictive cNTnC Conformations.

In addition to the protein receptor conformations used, the effect of different ligand preparation strategies on active compound enrichment was tested. To better emulate the conditions present when screening compounds in a large database which are typically provided as 2D structures (such as the NCI database), all 1007 ligands (1000 decoys and 7 actives) were converted into 2D structures prior to the preparation process. This was done in order to maintain consistency with

respect to how all of the ligands were treated. LigPrep was used for the preparation of the ligands.⁶⁰ This software allows the user to add hydrogen atoms, generate various ionization states at multiple pH values using either the built-in Ionizer or Epik ionization protocols,^{61,62} generate tautomers, generate alternative chiralities, and minimize the structure using a user-selected force field.^{63–66} Depending upon the inputs chosen, multiple versions of each ligand could be generated (e.g., versions with different protonation states). Table 1 lists the ligand preparation strategies that were tested along with the number of generated ligands.

Subsequently, the prepared active and decoy ligands were docked using Glide XP into each of the 35 prepared receptor conformations. Each ligand was docked into each of the prepared receptor conformations. The top scoring pose of each ligand along with its docking score were extracted from the Glide XP results and used for further analysis.

A ROC (receiver operator characteristic) curve analysis was performed to measure the relative predictive ability to find hydrophobic pocket binders of each protein conformation.⁶⁷ This method of analysis is used to evaluate how well a system predicts a binary classifier system. In this case, we were testing how well each specific protein conformation can predict the binding of known binders into the hydrophobic pocket. The ROC curves were generated by ranking the docking scores for all the active and decoy ligands for each receptor. The curve was created by plotting the number of true positives (TP) divided by the sum of true positives and false negatives (FN) versus the number of false positives (FP) divided by the sum of false positives and true negatives (TN). In other words, the occurrence of the active compounds is plotted against the occurrence of the decoys in the rank-ordered list of docking scores. The axes are normalized.

A total of 105 ROC curves were generated, resulting from the 35 receptor conformations tested in combination with each of the three ligand preparation methods. The curves were generated using an in-house python script that reads in the output docking scores, recording only the score of the top pose for each ligand. If the ligand preparation method generated multiple versions of a ligand, only the top scoring pose out of all the possible versions is extracted, resulting in a total list of 1007 docking scores. In many cases, if a ligand scored poorly, it was not reported in the Glide XP output file. This resulted in the total number of reported docked ligands being less than the actual number of ligands used as input. To account for this, we added the ligands that do not have reported scores onto the end of the list, while making the assertion that if any of those ligands were active compounds they would be placed at the very end. This was done to represent a “worst-case” scenario where the active ligands with unreported scores were assumed to dock worse than any of the unreported decoy ligands.

A combination of area under the curve (AUC) and enrichment factor was used to measure the relative predictive ability of each receptor. The AUC was calculated by rectangular integration. The enrichment factor for each receptor conformation/ligand preparation combination was calculated using

$$EF = \frac{N_{\text{active in top 40}}}{40} \times \frac{N_{\text{total}}}{N_{\text{actives}}} = \frac{N_{\text{active in top 40}}}{40} \times \frac{1007}{7}$$
$$= 3.596 \times N_{\text{active in top 40}}$$

where $N_{\text{active in top 40}}$ is the number of active compounds found in the top 40 (chosen based upon only being able to order a

maximum of 40 compounds at a time from the NCI) scoring ligands, N_{total} is the total number of docked ligands (actives + decoys, in this case a total of 1007 ligands), and N_{actives} is the total number of actives (in this case 7). Although pragmatic, the decision to use a sample set of 40 for the enrichment factor provides a large enough set to demonstrate enrichment as well as ensures feasibility for experimental follow-up. Alternative approaches have been explored for selecting the most suitable metrics, such as the null hypothesis protocol presented Hawkins and co-workers.⁶⁸ Unfortunately, due to the highly non-normal distribution of the enrichment factors, this null hypothesis method could not be applied. In theory, a perfectly random distribution of actives and decoys would result in a normalized AUC of 0.5 and an enrichment factor of 1, based upon the assumption that in a perfectly random system the active ligands would be evenly distributed throughout the scored compound list. Normally, the results would be compared against these metrics. However, since our ligand preparation strategies generally generated multiple versions of each ligand and only the top scoring of each ligand was used for the ROC curve, these baselines needed to be adapted for the respective ligand preparation strategies. To account for this, we developed an in-house python-based random docking score generator. The script read in the list of docked ligands for each receptor that contains the correct number of multiple versions of each and assigned each of them a random docking score ranging from 0 to 1 generated using a random number generator. AUCs and enrichment factors were calculated by extracting only the top scoring of each ligand resulting in a list of 1007 ligands. This process was repeated for thousands of iterations. The values for the AUC and the EF converged after ~50,000 iterations. Plots illustrating this convergence are shown in Figure S3 of the Supporting Information. The calculations were repeated 50,000 times and averaged to give an AUC and enrichment factor baseline that was specific to each receptor/ligand preparation method. The baselines were determined by averaging three trials of 50,000 iterations. The raw calculated AUC and enrichment factor values for each combination along with their respective baselines can be found in Table 1 of the Supporting Information.

Based upon the ROC curve results, three top receptor conformations were chosen along with a ligand preparation method. This was accomplished by comparing AUC and enrichment factor calculations for each receptor and ligand preparation combination to their respective baselines. A ligand preparation method was chosen first by identifying which set of 35 docking calculations had the most receptors with enrichment factors above their baselines. After selecting a ligand preparation method, three receptor conformations with the highest AUCs and enrichment factors compared to their respective baselines were chosen.

Virtual Screen of NCI Database. The entire National Cancer Institute (NCI) open database (265,242 total compounds) was used for the virtual screen. The compounds were prepared using the ligand preparation method identified as providing the best calcium sensitizer binding predicting capability (OPLS_2005 force field for minimization, the Ionizer ionization method to generate all possible structures at a target pH of 7.4, and generating all combinations of stereoisomers with at most five versions generated per ligand). This ligand preparation method generated a total of 513,446 compounds. Due to the large number of compounds in the database, the virtual screening workflow was used for the screening.⁶⁷ The

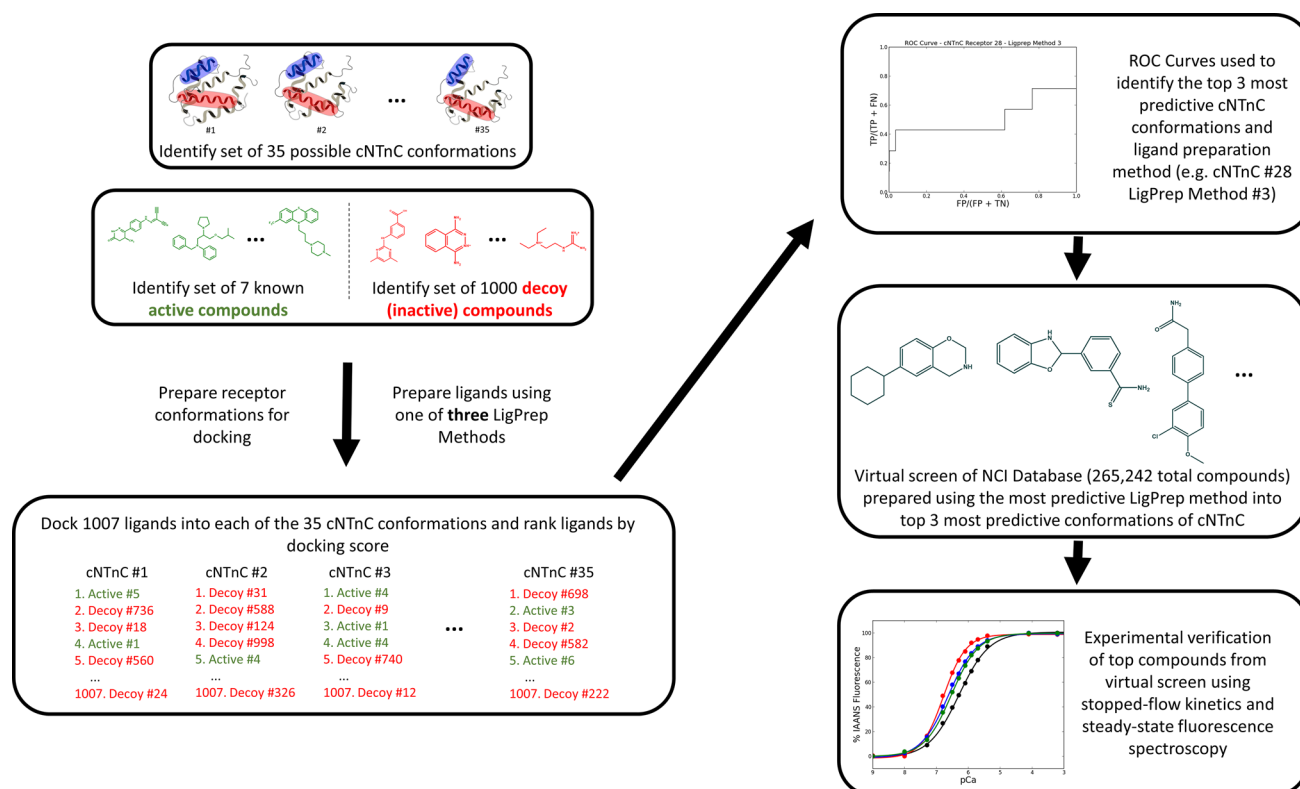


Figure 4. Drug discovery protocol.

compounds post-LigPrep were docked into each of the three cNTnC receptor conformations selected from the test set using Glide HTVS. From these results, the top 10% for each receptor (26,000 compounds for each of the three receptors; after ligand preparation: 54,685 for #16, 49,604 for #19, and 49,017 for #28) were then docked into the three receptors using Glide SP. Finally, the top 10% of the SP results for each receptor (2600 compounds for each of the three receptors; after ligand preparation: 6319 for #16, 5292 for #19, and 5734 for #28) were docked into all three receptors using Glide XP.

Using a custom python script, the results from the Glide XP docking for each receptor were analyzed. The script reported all compounds that appeared in the top 100 scoring for all three receptors, in addition to the top 15 scoring ligand poses for each receptor individually and the compounds in ranked order averaged across all three receptors. From these results, a set of compounds was chosen for experimental testing. One of the compounds appeared in the top 100 scoring for all three receptors, and the remaining compounds were chosen from the ranked list of averaged scores with preference being given to compounds that occurred in the top 15 of any of the three receptors.

In addition, a subset of the NCI database was also screened. This subset contained all the compounds from the database that are structurally similar to NSC147866 (Tanimoto index >80%), a previously determined calcium sensitizing agent found in the NCI database.²⁶ This subset contained a total of 336 compounds. Using the same method for ligand preparation, the ligands were docked into each of the top three receptors using Glide XP. The same script used for the entire database analysis was used. A check was added to ensure that there were no duplicates with the set determined from the entire database. Another set of compounds were selected from

this list. These compounds were ordered from the NCI Developmental Therapeutics Program (DTP) for potential experimental verification.

Based upon the experimental screening of a portion of the compounds using stopped flow, NSC600285 was identified as a potential Ca^{2+} sensitizer. A final screen was then performed on compounds structurally similar to NSC600285 (Tanimoto index > 80%). The subset contained 68 different compounds. The same procedure was followed as was used for NSC147866.

Proteins and Ligands Utilized for Experimental Verification. The pET3a plasmid-encoding human cardiac troponin C (cTnC) was a generous gift from Dr. Lawrence B. Smillie (University of Alberta, Edmonton, AB). The cTnC^{C35S} mutant was generated, expressed, purified, and labeled with environmentally sensitive fluorescent probe IAANS on Cys⁸⁴ as previously described.⁶⁹ The cTnI_{128–180} peptide was synthesized by The Ohio Peptide, LLC (Powell, OH). The cTnC-cTnI chimera (utilized for initial compound screening) was generated, expressed, purified, and labeled with IAANS on Cys⁵³ as previously described.⁷⁰

The ligands were obtained from the National Cancer Institute Developmental Therapeutics Program. The samples obtained ranged between 5 and 10 mg. Bepridil was purchased from Sigma-Aldrich. The samples were dissolved in DMSO to a stock concentration of 50 mM.

Steady-State Fluorescence Measurements. All steady-state fluorescent measurements were carried out using a PerkinElmer LS55 fluorescence spectrometer at 15 °C. IAANS fluorescence was excited at 330 nm and monitored at 450 nm as microliter amounts of CaCl_2 were added to 2 mL of IAANS-labeled cTnC^{C35S} (0.25 μM) in the presence of the cTnI_{128–180} peptide (1.25 μM), in the absence or presence of a compound (100 μM), in a titration buffer (200 mM MOPS (to

prevent pH changes upon addition of Ca^{2+}), 150 mM KCl, 2 mM EGTA, at pH 7.0), with constant stirring. $[\text{Ca}^{2+}]_{\text{free}}$ was calculated using the computer program EGCA02 developed by Robertson and Potter.⁷¹ The Ca^{2+} sensitivities were reported as a dissociation constant K_d , representing a mean of at least three separate titrations \pm SE. The data were fit with a logistic sigmoid function (mathematically equivalent to the Hill equation). As a control against potential aggregation, the above measurements were repeated in the presence of 0.025% zwitterionic detergent Tween-80.

Stopped-Flow Fluorescence Measurements. All kinetic measurements were carried out using an Applied Photophysics Ltd. (Leatherhead, UK) model SX.18MV stopped-flow apparatus with a dead time of ~ 1.4 ms. IAANS fluorescence was excited at 330 nm with emission monitored through a 420–470 nm band-pass interference filter (Oriel, Stratford, CT). EGTA (10 mM) in a stopped-flow buffer (10 mM MOPS, 150 mM KCl, at pH 7.0) was utilized to remove Ca^{2+} (500 μM) from IAANS labeled cTnC^{C35S} (0.5 μM) in the presence of a cTnI_{128–180} peptide (2.5 μM in the stopped-flow buffer at 15 °C. Here, 100 μM of each compound was individually added to both stopped-flow reactants to screen the compounds. The data were fit using a program (by P.J. King, Applied Photophysics Ltd.) that utilizes the nonlinear Levenberg–Marquardt algorithm. Each k_{off} represents an average of at least three separate experiments \pm SE, each averaging at least five shots fit with a single exponential equation.

Statistics. Experimental results obtained from the steady-state Ca^{2+} binding as well as the Ca^{2+} dissociation rates were compared by a one-way ANOVA followed by a Tukey's HSD (honest significant difference) posthoc test. A value of $p < 0.05$ was statistically significant.

RESULTS AND DISCUSSION

Previous studies using computer-aided drug discovery targeting cTnC have used either experimental cTnC structures (from X-ray crystallography or NMR) or geometrically representative snapshots from molecular dynamics simulations as receptors.²⁶ However, the cTnC conformations used in the virtual screens were never selected based upon their ability to correctly predict known cTnC binders. In this study, prior to performing any type of virtual drug screening, we ensured that the static protein conformations to be used as receptors were predictive of binding calcium-sensitizing compounds. The test sets of cTnC and cTnC-cTnI_{144–163} conformations, totaling 35 structures, were chosen from a combination of experimental crystal/NMR structures obtained from the protein databank and frames extracted from a molecular dynamics trajectory of an NMR complex of DFBP-O bound cTnC-cTnI_{144–163} (PDB 2L1R). Figure 4 summarizes our drug discovery protocol.

Generation of an Ensemble of cTnC Conformations That Represent the Structural Flexibility of the Hydrophobic Patch. A preselection of cTnC and cTnC-cTnI_{144–163} conformations that represent the structural ensemble of cardiac TnC in solution was made to subsequently identify which of those conformations is most predictive for drug discovery. A total of five crystal/NMR structures were selected, all of which contain an active compound bound to either cTnC or cTnC-cTnI_{144–163}. Three of these conformations have actives bound to cTnC-cTnI_{144–163}: 1XLF [contains bepridil],⁵⁰ 2KRD [contains w7],⁵¹ and 2L1R [contains DFBP-O].²⁹ The other conformations contain active

ligands that are bound to just cTnC: 1WRK [contains trifluoperazine]²⁸ and 2KFX [contains w7].⁵² The coordinates for the docking location were chosen as the central coordinates of the docked ligand in each respective structure. These conformations account for receptors #1–5.

The remaining 30 structures were extracted from a MD simulation of DFBP-O bound cTnC-cTnI_{144–163} (PDB 2L1R). Using POVME, the pocket volume for each frame corresponding to every 20 ps of the 100 ns trajectory was calculated. The volumes plotted as a function of time are shown in Figure 5. Fifteen frames were chosen that have volumes

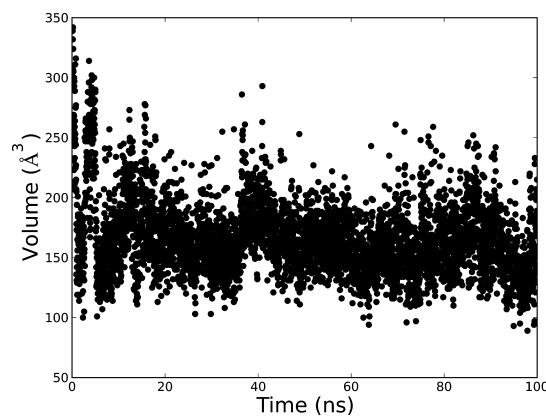


Figure 5. Hydrophobic patch pocket-volumes calculated every 20 ps of a 100 ns MD trajectory of cTnC-cTnI_{144–163}. Volumes, in units of Å^3 , were calculated using POVME.

ranging from 106–258 Å^3 and were dispersed evenly throughout the trajectory. The selection of larger pockets in the MD simulation was based on reports that screening of larger pocket conformations has been associated with improved outcomes in drug discovery.^{72,73} The volumes and relative RMSDs of each of these 15 conformations are shown in Table 2. These defined structures #6–20. The final 15 structures, #21–35, were extracted from the MD trajectory using a cluster analysis. The details of the RMSD cluster analysis can be found

Table 2. Results of Pocket-Volume Analysis of Receptor Conformations Selected from the 100 ns MD Simulation of cTnC-cTnI_{144–163}^a

Receptor	Volume (Å^3)	RMSD Compared to 2L1R (Å)
6	236	4.273
7	258	4.170
8	219	4.203
9	244	4.575
10	176	4.622
11	176	4.638
12	130	5.236
13	206	5.254
14	144	5.169
15	226	4.928
16	171	4.814
17	163	4.986
18	187	4.993
19	106	4.891
20	219	4.612

^aCalculations were performed using POVME. RMSD calculations were performed over the entire cTnC-cTnI_{144–163} complex.

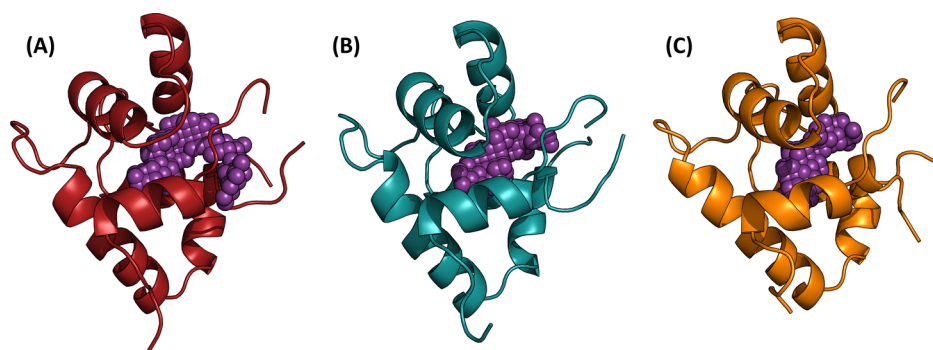


Figure 6. Three cNTnC-cTnI_{144–163} conformations identified as most predictive of ligand binding to the cNTnC hydrophobic pocket: (A) receptor #16, (B) receptor #19, and (C) receptor #28. The hydrophobic pockets are depicted by the purple spheres.

in a previous paper.²⁶ The docking site location for receptors #6–35 was chosen as the central coordinates of the bound DFBP-O in the initial frame of the MD simulation.

The 35 receptor conformations selected for the test set are structurally similar but have varying properties making them all excellent candidates. The RMSDs (calculated to the experimental structure 2L1R) range from 3.08 to 5.88 Å over residues 1–89 and from 2.32 to 3.70 Å over just helices A and B. Because all of the receptor conformations initially contained a bound ligand, helices A and B are in an open conformation, thus creating a sizable hydrophobic pocket. This is necessary for further virtual drug screening as there needs to be enough volume in the pocket to accommodate ligands of variable sizes.

Selection of a Ligand Preparation Method and Three cNTnC Conformations That Most Accurately Predict Binding of Known cNTnC Binders. Following the assembly of an ensemble of 35 representative cNTnC and cNTnC-cTnI_{144–163} conformations, we used knowledge about known cTnC binders to identify 3 out of the 35 cNTnC conformations that have the highest predictive value for cNTnC binding. We docked known cNTnC binders and decoy ligands into all 35 cNTnC conformations and then selected the three conformations that ranked known ligands best with respect to decoys (Figure 6).

In addition to the protein receptor conformations used, it was important to use a ligand preparation method that gives ligand structures that are highly predictive of binding to the hydrophobic pocket in cNTnC. Several of the ligand databases that are commonly used for virtual drug screening often only provide ligands as 2D structures that generally do not encode the correct ionization state or chirality. Using LigPrep,⁶⁰ three different ligand preparation methods were tested on the 7 active ligands and 1000 decoy ligands. A list of the methods tested is shown in Table 1. The total ligand test set (1007 total ligands) was docked into each of the 35 cNTnC and cNTnC-cTnI_{144–163} conformations in the test set and the docked ligands were ranked by their docking score.

For each ligand preparation method and cNTnC conformation, a ROC curve was generated that assesses how well-known active ligands can be ranked in relation to inactive decoys for that particular ligand preparation method and receptor cNTnC conformation (Supporting Information, Figure S4). This allowed identification of particular cNTnC conformations that are most predictive of finding known cNTnC binders, i.e., conformations that rank the active compounds higher compared to the decoys. The area under the ROC curve (AUC) and an enrichment factor were

calculated for each receptor conformation/ligand preparation method pair and compared to a baseline specific to each system. Typically, a ROC curve has an AUC baseline of 0.5 and enrichment factor of 1 (both of which demonstrate the system being evenly distributed). In this case, each system's baseline value had to be adjusted since the ligand preparation methods used generated multiple versions of the same ligand (various ionization states for example). This was accomplished by averaging the AUC and enrichment factors over 50,000 test runs using random docking scores. The results from these calculations are shown in Table 3. AUCs and enrichment factors above the respective baseline values are an indication of how well a particular system (composed of both the receptor conformation and ligand preparation method) can predict true active ligand binding to the hydrophobic pocket of cNTnC. These two metrics were used to determine the optimal ligand preparation method along with three representative cNTnC conformations.

The ligand preparation method found to have the most receptors with enrichment factors above their respective baselines was LigPrep Method 3 (Table 3). This method used the OPLS_2005 force field for minimization, the Ionizer ionization method to generate all possible structures at a target pH of 7.4, and generated all combinations of stereoisomers with at most five versions generated per ligand. This ligand preparation method was chosen as the method to be used for the prospective virtual screening to identify novel calcium sensitizing agents.

Within LigPrep Method 3, each of the individual receptors' ROC curves were analyzed. The three receptors chosen as most predictive of active binding (receptors #16, #19, and #28) were selected based upon how far their respective AUCs and enrichment factors were above the respective baselines. The relative AUC values for each of these three receptors are 0.12, 0.08, and 0.04. Most critical in the selection of these particular receptor conformations were the enrichment factors. The respective enrichment factors for each receptor were 2.42, 2.56, and 9.55. Receptor #28 exhibited the largest enrichment factor indicating that it had ranked the most active compounds within the top 40 docked ligands. These other two receptors also had elevated enrichment factors when compared to their respective baselines. Receptors #16 and #19 were extracted from the pocket-volume analysis, while receptor #28 originated from the RMSD cluster analysis of the MD simulation of DFBP-O bound cNTnC-Ca²⁺-cTnI_{144–163} (PDB 2L1R). The three receptors chosen for the virtual screen are shown in Figure 6. The pairwise RMSDs for the three receptor conformations

Table 3. ROC Curve Results for LigPrep Methods 1, 2, and 3 and Receptors #1–35^a

Receptor	LigPrep Method 1		LigPrep Method 2		LigPrep Method 3	
	Relative AUC	Relative EF	Relative AUC	Relative EF	Relative AUC	Relative EF
1	-0.07	-0.80	0.16	-0.74	0.09	-1.72
2	-0.02	-0.94	-0.12	-0.86	-0.20	-1.80
3	0.06	6.26	0.09	-0.84	0.06	2.15
4	0.06	-0.93	0.00	-0.84	-0.13	1.82
5	-0.02	-0.94	-0.03	-0.85	-0.16	-1.79
6	0.03	-0.81	0.09	-0.74	0.13	-1.15
7	0.06	2.78	0.16	-0.66	0.11	-1.31
8	0.00	2.78	0.15	2.95	-0.01	2.27
9	0.15	6.22	0.10	-0.90	-0.04	1.66
10	0.21	6.56	0.22	2.70	0.12	2.02
11	0.15	-0.68	0.07	-0.87	0.00	2.20
12	0.15	-0.63	0.12	-0.64	0.11	2.39
13	0.15	2.89	0.14	2.70	0.03	1.95
14	0.13	2.76	0.12	2.72	0.02	1.85
15	-0.10	2.64	-0.01	-0.86	-0.13	-1.81
16	0.10	-0.82	0.16	-0.66	0.12	2.42
17	0.08	-0.85	0.12	-0.78	-0.01	-1.51
18	0.00	-0.86	0.07	-0.80	-0.05	-1.47
19	0.06	3.12	0.09	3.08	0.08	2.56
20	0.02	-0.94	0.05	-0.86	-0.06	-1.83
21	-0.07	-0.94	-0.12	-0.86	-0.18	-1.82
22	0.12	-0.60	0.14	-0.60	0.09	-0.87
23	0.19	-0.72	0.20	-0.70	0.06	-1.34
24	-0.14	-0.95	-0.13	-0.77	-0.15	-1.74
25	-0.15	-0.95	-0.07	-0.85	-0.08	-1.81
26	0.00	-0.97	0.02	-0.87	-0.04	-1.78
27	-0.05	-0.94	-0.07	-0.85	-0.07	1.80
28	0.04	-0.82	0.10	6.40	0.04	9.55
29	0.15	-0.75	0.18	-0.74	0.11	2.27
30	-0.07	-0.55	-0.04	-0.54	-0.01	-1.18
31	-0.06	-0.44	0.04	-0.23	0.00	-0.58
32	0.10	2.87	0.11	-0.70	0.02	-1.26
33	0.04	-0.94	0.12	2.75	-0.03	1.94
34	-0.05	-0.95	-0.01	-0.86	-0.01	-1.81
35	-0.02	-0.94	0.01	2.75	-0.08	1.79
Total Positive	22	10	25	8	17	16

^aThe reported areas under the curve and enrichment factors are relative to the baselines calculated for each ligand preparation method/receptor conformation pair. The receptors and the corresponding ligand preparation methods used for the virtual screening are bolded and italicized.

were 3.173, 3.274, and 3.498 Å, respectively. The pocket volumes for the three receptors, as calculated with POVME, were 171, 106, and 108 Å³, respectively. These volumes fall within the range of volumes for the receptor conformations in the test set extracted from the MD trajectory. The lack of distinguishing features among the three chosen receptor conformations demonstrates the value of the ROC analysis. Without said analysis, there was no obvious reason to select the conformations that were selected. All three receptors selected originated from the MD simulation with DFBP-O bound and were complexed with the switch peptide, cTnI_{144–163}. The lack of experimental structures in this final set of the three most predictive cNTnC conformations underscores the importance of using MD in accounting for receptor flexibility in virtual screening. Encouragingly, in both receptors #19 and #28,

DFBP-O appeared in the list of top 40 docking score compounds. This is indicative of these conformations having a high predictive value for predicting active docking.

Virtual Screen To Identify Novel Calcium-Sensitizing Agents. After identification of a predictive ligand preparation method and three predictive cNTnC conformations, we performed virtual screening of the entire NCI database using Schrödinger's virtual screening workflow to identify novel compounds that are potential Ca²⁺ sensitizers for cNTnC. We hypothesized that using this particular combination of three receptor conformations and ligand preparation method in the virtual screen would increase the chances of identifying active calcium-sensitizing molecules that bind to the hydrophobic pocket. The receptor conformations and ligand preparation method used for the compounds in the database were identified as being highly predictive of binding to the hydrophobic pocket.

The virtual screen was performed by docking all compounds first using Glide HTVS, then docking the top 10% for each receptor using Glide SP, and then finally docking the top 10% of those using Glide XP. After the virtual screening, a set of the top scoring compounds were chosen. These compounds were based on analyzing the average docking score across all three receptor conformations as well as identifying compounds that occurred in the top 100 scoring for all three receptor conformations. The selection was based on compounds having good scores in all three receptor conformations. Only a single compound (NSC254212) was found in the top 100 of all three receptor conformations and coincidentally had the best average docking score. The remaining compounds were chosen from the ranked list of averaged scores with preference being given to compounds that occurred in the top 15 of any of the three receptors. A second screen was performed on compounds within the NCI database that were structurally similar to NSC147866, a compound that we recently identified to be a weakly binding calcium sensitizer. We hypothesized that a derivative of NSC147866 might have a high probability of binding to the hydrophobic pocket. The compounds chosen were also filtered based upon availability for ordering from the NCI DTP. Only compounds that were available for ordering were chosen. The compounds selected along with their molecular weights and average docking scores (across all three receptors) are shown in Table 4.

A final screen was performed on compounds from the NCI database that were structurally similar to NSC600285, a compound that was identified from the initial set of compounds to bind cNTnC and show calcium-sensitizing properties (see Experimental Verification section for details). Based upon this screen, additional compounds were selected using the same selection methodology used for the other screens.

Samples of the compounds (5–10 mg of each) identified through the virtual screening process were ordered from the NCI DTP. The compounds were screened using stopped-flow, and the two promising candidates were subsequently tested for their ability to act as calcium sensitizers. Partly because of solubility issues and inner filter effects, only a portion of the compounds were successfully screened.

Experimental Verification. The two potential Ca²⁺ sensitizers (NSC600285 and NSC611817) were initially identified via stopped-flow screening using the cTnC-cTnI chimera.⁷⁰ Since changes in Ca²⁺ sensitivity can be caused by either changes in Ca²⁺ dissociation or association rate, or a combination of both rates, we needed to determine whether the

Table 4. Top Results from Virtual Drug Screenings of the NCI Database and Both Subsets of the NCI Database^a

Initial Screen of Compounds			Screen of Compounds Similar to NSC600285		
NSC	Avg. Docking Score	Molecular Weight (g/mol)	NSC	Avg. Docking Score	Molecular Weight (g/mol)
254212	-10.09	339.27	611817	-10.21	256.30
600285	-7.69	272.30	611815	-10.16	258.27
600286	-7.58	256.30	611816	-10.05	272.30
24047	-6.79	300.40	603663	-9.77	302.33
24045	-6.73	286.38	93367	-9.19	272.30
67598	-6.45	248.33	26182	-8.21	412.48
202117	-6.42	285.41	600291	-6.08	300.35
170630	-6.25	270.33	157109	-5.78	390.48
77134	-6.14	259.35	605546	-5.65	368.39
671841	-5.98	232.71	628872	-4.03	344.36
34046	-5.95	252.36	27593	-3.68	410.47
269897	-5.76	224.30	102052	-2.70	328.36
19841	-5.56	198.27	681610	-2.66	284.31
147896	-5.07	304.39	27594	-2.55	438.52
			55274	-2.54	330.34
			16317	-1.77	240.30

^aThe initial screen comprised the entire NCI Database and the subset of compounds similar to NSC147866. Shown are the NSC identification numbers of each compound along with their average docking score over the three receptors as well as their molecular weight.

two compounds were in fact Ca²⁺ sensitizers. The effects of the compounds on Ca²⁺ sensitivity of cTnC in the presence of cTnI_{128–180} were measured by following the Ca²⁺-induced changes in fluorescence of IAANS-labeled cTnC^{C35S} using steady-state fluorescence titrations. We determined that both compounds led to an increase in calcium sensitivity of IAANS-labeled cTnC^{C35S} in the presence of cTnI_{128–180} (Figure 7A). The increase in Ca²⁺ sensitivity is apparent by the left shift (decrease in K_d) of the steady-state curves. A one-way ANOVA followed by a Tukey's HSD analysis indicated that both compounds show a statistically significant increase in calcium sensitivity when compared to the control.

We also compared the Ca²⁺-sensitizing effects of the two new compounds to that of a known Ca²⁺ sensitizer, bepridil.⁷⁴ Ca²⁺ induced increases in IAANS fluorescence, which occur when Ca²⁺ binds to the regulatory N-domain of IAANS-labeled cTnC^{C35S} in the presence of cTnI_{128–180} and in the absence or presence of NSC600285, NSC611817, or bepridil are shown in Figure 7A. In the presence of cTnI_{128–180}, the IAANS-labeled cTnC^{C35S} exhibited a half-maximal Ca²⁺-dependent increase in IAANS fluorescence at 0.60 ± 0.03 μM. NSC600285, NSC611817, and bepridil led to ~2.4-, 2.1-, and 2.0-fold increases, respectively, in the Ca²⁺ sensitivity of the IAANS-labeled cTnC^{C35S} in the presence of cTnI_{128–180}. Statistical analysis using a combination of one-way ANOVA and Tukey's HSD test indicated that the Ca²⁺-sensitizing effects of the two new compounds was similar to that of the known compound, bepridil. The Hill coefficients (steepness) for all the curves fell within 1.03 to 1.13, indicating a noncooperative binding event.⁷⁵

To confirm the initial stopped-flow screening results, further stopped-flow experiments were conducted to determine the effect of the two identified compounds on the kinetics of Ca²⁺ dissociation from cTnC in the presence of cTnI_{128–180}. Effects

were also compared to that of bepridil. Figure 7B shows that excess EGTA removed Ca²⁺ from the regulatory N-domain site of IAANS-labeled cTnC^{C35S} in the presence of cTnI_{128–180} at ~106 ± 2 s⁻¹. NSC600285, NSC611817, and bepridil led to ~2.5-, 2.3-, and 1.7-fold decelerations in the rate of Ca²⁺ dissociation from IAANS-labeled cTnC^{C35S} in the presence of cTnI_{128–180}. Statistical analysis using one-way ANOVA and Tukey's HSD test showed that all three compounds significantly slowed the rate of Ca²⁺ dissociation from IAANS-labeled cTnC^{C35S} in the presence of cTnI_{128–180}. Furthermore, the two new compounds led to a significantly slower Ca²⁺ dissociation from IAANS-labeled cTnC^{C35S} compared to that of bepridil. Our results indicate that the Ca²⁺ sensitization caused by all three compounds was largely due to deceleration in the Ca²⁺ dissociation rate.

The two compounds were filtered against the PAINS moieties (Pan Assay Interference Compounds) to ensure that both compounds were true positives.⁷⁶ PAINS compounds are compound moieties that are frequent hits in high throughput drug screens and have properties that lead to apparent activity in multiple assays.⁷⁷ NSC600285 and NSC611817 were analyzed using the FAFDrugs4 program utilizing filters for all three classes of PAINS compounds.^{78–80} Both compounds were identified as intermediate molecules due to the catechol functional group.^{81,82} Compounds with this functional group can potentially aggregate and provide indeterminate experimental results.

In order to show that NSC600285 and NSC611817 are displaying true activity and are not aggregating, we repeated the Ca²⁺ titrations in the presence of the zwitterionic detergent Tween-80 (0.025%) as recommended to rule out potential PAINS effects.⁸³ In the presence of Tween-80, both compounds still statistically Ca²⁺ sensitized cTnC^{C35S} in the presence of cTnI_{128–180} (Figure 7C). Additionally, we measured the effect of the compound NSC603663 which did not pass our initial screening since it did not affect the rate of Ca²⁺ dissociation from the cTnC-cTnI chimera. Compound NSC603663 was selected because it also contains a catechol group. Figure 7D demonstrates that NSC603663 did not Ca²⁺ sensitize cTnC^{C35S} in the presence of cTnI_{128–180}. Thus, the presence of the catechol group by itself is not sufficient to affect our assay.

In addition to potential aggregation, the catechol groups in the compounds pose the potential to oxidize and form ortho-quinones. Docking calculations were performed on the oxidized forms of NSC600285 and NSC611817. The docking scores averaged over all three receptors for the unoxidized (catechol) forms of NSC600285 and NSC611817 were -7.69 and -10.21, respectively. The oxidized (ortho-quinone) forms gave significantly worse docking scores of -4.90 and -6.23, respectively, strongly suggesting that the unoxidized group is the dominant bound form. Should these compounds be developed further, additional experiments need to be performed to verify the binding of the unoxidized and oxidized forms, and this will be explored in future work.

The two compounds identified, NSC600285 and NSC611817, belong to a class of isoflavans and have been previously discovered as being potential inhibitors for human lipoxygenases (hLO).⁸⁴ Both compounds were identified as demonstrating high selectivity and potency for 15-hLO-1 (reticulocyte 15-human lipoxygenase-1, which has been implicated in atherogenic processes)^{85,86} and inhibition of 12-hLO (platelet 12-human lipoxygenase). Thus, in addition to the

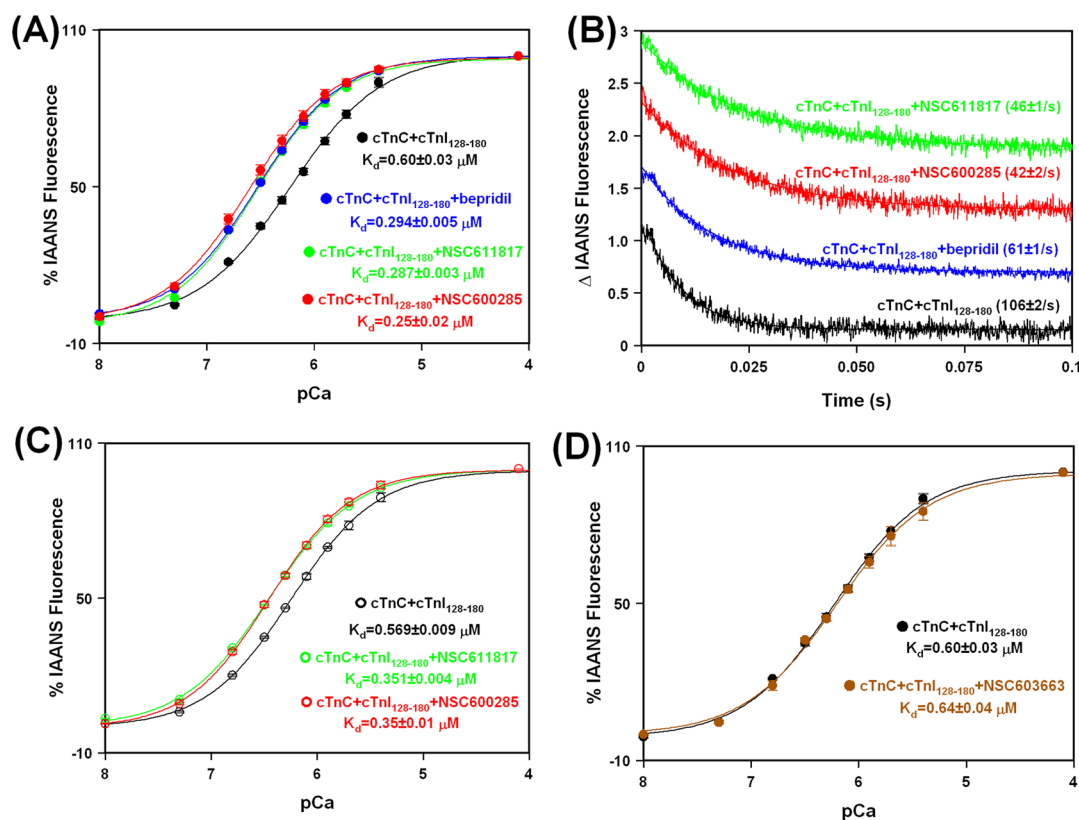


Figure 7. Effect of NSC600285, NSC611817, and bepridil on the Ca²⁺ binding properties of cTnC in the presence of cTnI₁₂₈₋₁₈₀. (A) Plot of the steady-state Ca²⁺ titrations performed in the absence or presence of compounds NSC600285, NSC611817, or bepridil in the absence of the detergent Tween-80. This panel shows increases in IAANS fluorescence, which occur as Ca²⁺ binds to IAANS-labeled cTnC^{C35S} (0.25 μM) in the presence of cTnI₁₂₈₋₁₈₀ (1.25 μM) or in the absence or presence of 100 μM of NSC600285, NSC611817, or bepridil at 15 °C. The IAANS fluorescence was excited at 330 nm and monitored at 450 nm. (B) Time course of decreases in IAANS fluorescence measured in a stopped-flow apparatus as Ca²⁺ was removed by excess EGTA (10 mM) in the absence or presence of 100 μM of NSC600285, NSC611817, or bepridil, from IAANS-labeled cTnC^{C35S} (0.5 μM) in the presence of cTnI₁₂₈₋₁₈₀ (2.5 μM), and in the absence or presence of 100 μM of NSC600285, NSC611817, or bepridil at 15 °C. Each trace is an average of at least five stopped-flow shots fit with a single exponential equation. The traces have been normalized and staggered for clarity. The IAANS fluorescence was excited at 330 nm and monitored through a 420–470 band-pass interference filter. (C) Results from experiments identical to those in panel A but this time in the presence of the detergent Tween-80. This panel shows increases in IAANS fluorescence, which occur as Ca²⁺ binds to IAANS-labeled cTnC^{C35S} (0.25 μM) in the presence of cTnI₁₂₈₋₁₈₀ (1.25 μM) and in the absence or presence of 100 μM of NSC600285 or NSC611817 at 15 °C all in the presence of 0.025% Tween-80. (D) Plot of the steady-state Ca²⁺ titrations performed in the absence or presence of compound NSC603663 and in the absence of the detergent Tween-80. This panel shows increases in IAANS fluorescence, which occur as Ca²⁺ binds to IAANS-labeled cTnC^{C35S} (0.25 μM) in the presence of cTnI₁₂₈₋₁₈₀ (1.25 μM) and in the absence or presence of 100 μM of NSC603663 at 15 °C.

Ca²⁺ sensitization, these compounds could also be beneficial for the treatment of heart failure via inhibition of 15-hLO-1 and 12-hLO.⁸⁷

CONCLUSION

In this study, the relaxed complex scheme (RCS) was employed to identify novel compounds that increase calcium sensitization of cTnC. In contrast to previous studies, in preparation for the virtual screening, cTnC conformations were identified based on their ability to correctly predict known cTnC binders. The large NCI DTP database was subsequently screened against those particular cTnC conformations, and 40 compounds were ordered for testing. A portion of the compounds identified in the virtual screen (30 total) were tested using stopped-flow kinetics, and two of the compounds that were found to show Ca²⁺-sensitizing properties were then tested using steady-state fluorescence titrations. Using this methodology, we have successfully identified two novel compounds, NSC600285 and NSC611817, both of which showed increased calcium sensitization (~2.4 fold) and a

slowed calcium dissociation rate (~2.5 fold). These effects on the rate of Ca²⁺ dissociation are stronger than for bepridil, a known calcium sensitizer. Titration experiments in the presence of detergent Tween-80 ruled out the possibility of false positive assay results due to aggregation caused by the catechol functional groups. The chemical structures of NSC600285 (3-(4-methoxyphenyl)-6,7-chromanediol) and NSC611817 (3-(4-methylphenyl)-7,8-chromanediol) are shown in Figure 8. We speculate that the 3-phenylchromane scaffold, which contains the pharmacophore chromane (a heterocyclic compound also known as benzodihydropan), is crucial in cTnC binding and calcium sensitization. These compounds had average docking

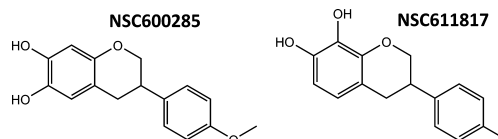


Figure 8. Chemical structures of NSC600285 and NSC611817.

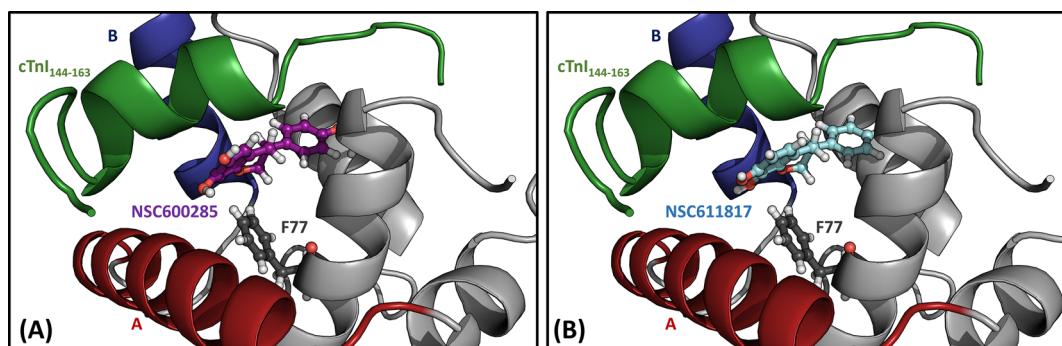


Figure 9. Docked poses of NSC600285 (A) and NSC611817 (B) in conformation #28 of cNTnC-cTnI₁₄₄₋₁₆₃ with the residue F77 depicted.

scores into the three receptor conformations chosen through the RCS of -7.69 and -10.21 , respectively. For both compounds, the docking results show that there is a T-shaped π - π interaction between the chromane portion and Phe 77 in cNTnC. NSC600285 also shows hydrogen bonding with the backbone of Ala 95. The docked poses of these compounds along with Phe 77 are depicted in Figure 9. NSC600285 was selected from the screen of the entire database, and NSC611817 was selected from the subsequent screen of compounds structurally similar to NSC600285. Both compounds have low Tanimoto similarity coefficients when compared to the seven known active compounds. The maximum common substructure Tanimoto similarity coefficients, as calculated using ChemMine Tools,⁸⁸ ranged from 17% to 39% for NSC600285 and 18% to 36% for NSC611817. This suggests that the relaxed complex scheme in combination with the identification of conformations that are predictive of binding was successful in identifying truly novel compounds. We would have never screened NSC600285 and NSC611817 based on their similarity to other known active compounds. Finally, despite the successful identification of a novel pharmacophore and two calcium sensitizers, solubility proved to be a limiting factor in the experimental verification (several of the compounds screened experimentally could not be tested due to severe solubility issues). It is not surprising that the virtual screen proposes hydrophobic compounds to bind to the hydrophobic pocket of troponin C. However, this suggests that successful compounds need to exhibit a delicate balance between hydrophobic and hydrophilic groups. Future work will focus on including predicted solubility into the virtual screen to dramatically increase the number of compounds that can be tested experimentally.

In conclusion, we have identified two novel Ca^{2+} sensitizers, NSC600285 and NSC611817. The Ca^{2+} sensitization effects of the two compounds were largely due to the slower rate of Ca^{2+} dissociation. Thus, the use of our relaxed complex scheme and virtual screening in combination with experimental verification shows great promise in discovering new compounds that could one day be used to treat heart disease.

■ ASSOCIATED CONTENT

● Supporting Information

The Supporting Information is available free of charge on the ACS Publications website at DOI: 10.1021/acs.jcim.7b00536.

Additional figures and detailed ROC curve results. (PDF)

■ AUTHOR INFORMATION

Corresponding Author

*Phone: 614-292-8284. Fax: 614-292-1685. E-mail: lindert.1@osu.edu.

ORCID

Steffen Lindert: 0000-0002-3976-3473

Funding

Research reported in this publication was supported in part by the NIA of NIH under Award Number R03 AG054904 (to S.L.) and the NHLBI of NIH under Award Number R01 HL132213 (to J.P.D.) and R01 HL138579 (to J.P.D.). The content is solely the responsibility of the authors and does not necessarily represent the official views of the NIH.

Notes

The authors declare no competing financial interest.

■ ACKNOWLEDGMENTS

The authors thank the members of the Lindert group for useful discussions and Dr. Jalal Siddiqui for the generation of the cTnC-cTnI chimera used in the initial experimental screening. We thank the Ohio Supercomputer Center for valuable computational resources.⁹⁰

■ REFERENCES

- (1) Biesiadecki, B. J.; Davis, J. P.; Ziolo, M. T.; Janssen, P. M. L. Tri-modal regulation of cardiac muscle relaxation; intracellular calcium decline, thin filament deactivation, and cross-bridge cycling kinetics. *Biophys. Rev.* **2014**, *6*, 273–289.
- (2) Katrukha, I. A. Human cardiac troponin complex. Structure and functions. *Biochemistry (Moscow)* **2013**, *78*, 1447–1465.
- (3) Marks, A. R. Calcium and the heart: a question of life and death. *J. Clin. Invest.* **2003**, *111*, 597–600.
- (4) Gordon, A. M.; Homsher, E.; Regnier, M. Regulation of contraction in striated muscle. *Physiol Rev.* **2000**, *80*, 853–924.
- (5) Kobayashi, T.; Jin, L.; de Tombe, P. P. d. Cardiac thin filament regulation. *Pfluegers Arch.* **2008**, *457*, 37–46.
- (6) Filatov, V. L.; Katrukha, A. G.; Bulargina, T. V.; Gusev, N. B. Troponin: structure, properties, and mechanism of functioning. *Biochemistry. Biokhimiia* **1999**, *64*, 969–985.
- (7) Tikunova, S. B.; Davis, J. P. Designing Calcium-sensitizing Mutations in the Regulatory Domain of Cardiac Troponin C. *J. Biol. Chem.* **2004**, *279*, 35341–35352.
- (8) Lindert, S.; Kekenus-Huskey, P. M.; McCammon, J. A. Long-Timescale Molecular Dynamics Simulations Elucidate the Dynamics and Kinetics of Exposure of the Hydrophobic Patch in Troponin C. *Biophys. J.* **2012**, *103*, 1784–1789.
- (9) Williams, M. R.; Lehman, S. J.; Tardiff, J. C.; Schwartz, S. D. Atomic resolution probe for allostery in the regulatory thin filament. *Proc. Natl. Acad. Sci. U. S. A.* **2016**, *113*, 3257–3262.

- (10) Li, M. X.; Hwang, P. M. Structure and function of cardiac troponin C (TNNC1): Implications for heart failure, cardiomyopathies, and troponin modulating drugs. *Gene* **2015**, *571*, 153–166.
- (11) Scholz, H. Inotropic drugs and their mechanisms of action. *J. Am. Coll. Cardiol.* **1984**, *4*, 389–397.
- (12) Francis, G. S.; Bartos, J. A.; Adaya, S. Inotropes. *J. Am. Coll. Cardiol.* **2014**, *63*, 2069–2078.
- (13) Hasenfuss, G.; Teerlink, J. R. Cardiac inotropes: current agents and future directions. *Eur. Heart J.* **2011**, *32*, 1838–1845.
- (14) Pollesello, P.; Papp, Z.; Papp, J. G. Calcium sensitizers: What have we learned over the last 25 years? *Int. J. Cardiol.* **2016**, *203*, 543–548.
- (15) Shettigar, V.; Zhang, B.; Little, S. C.; Salhi, H. E.; Hansen, B. J.; Li, N.; Zhang, J.; Roof, S. R.; Ho, H.-T.; Brunello, L.; Lerch, J. K.; Weisleder, N.; Fedorov, V. V.; Accornero, F.; Rafael-Fortney, J. A.; Gyorke, S.; Janssen, P. M. L.; Biesiadecki, B. J.; Ziolo, M. T.; Davis, J. P. Rationally engineered Troponin C modulates in vivo cardiac function and performance in health and disease. *Nat. Commun.* **2016**, *7*, 10794.
- (16) Papp, Z.; Édes, I.; Fruhwald, S.; De Hert, S. G.; Salmenperä, M.; Leppikangas, H.; Mebazaa, A.; Landoni, G.; Grossini, E.; Caimmi, P.; Morelli, A.; Guarracino, F.; Schwinger, R. H. G.; Meyer, S.; Algotsson, L.; Wikström, B. G.; Jørgensen, K.; Filippatos, G.; Parissis, J. T.; González, M. J. G.; Parkhomenko, A.; Yilmaz, M. B.; Kivikko, M.; Pollesello, P.; Follath, F. Levosimendan: Molecular mechanisms and clinical implications: Consensus of experts on the mechanisms of action of levosimendan. *Int. J. Cardiol.* **2012**, *159*, 82–87.
- (17) Haikal, H.; Kaivola, J.; Nissinen, E.; Wall, P. I.; Levijoki, J.; Lindén, I.-B. Cardiac troponin C as a target protein for a novel calcium sensitizing drug, levosimendan. *J. Mol. Cell. Cardiol.* **1995**, *27*, 1859–1866.
- (18) Hasenfuss, G.; Pieske, B.; Castell, M.; Kretschmann, B.; Maier, L. S.; Just, H. Influence of the Novel Inotropic Agent Levosimendan on Isometric Tension and Calcium Cycling in Failing Human Myocardium. *Circulation* **1998**, *98*, 2141–2147.
- (19) Sorsa, T.; Heikkinen, S.; Abbott, M. B.; Abusamhadneh, E.; Laakso, T.; Tilgmann, C.; Serimaa, R.; Annala, A.; Rosevear, P. R.; Drakenberg, T.; Pollesello, P.; Kilpeläinen, I. Binding of Levosimendan, a Calcium Sensitizer, to Cardiac Troponin C. *J. Biol. Chem.* **2001**, *276*, 9337–9343.
- (20) Pollesello, P.; Ovaska, M.; Kaivola, J.; Tilgmann, C.; Lundström, K.; Kalkkinen, N.; Ulmanen, I.; Nissinen, E.; Taskinen, J. Binding of a new Ca²⁺ sensitizer, levosimendan, to recombinant human cardiac troponin C. A molecular modelling, fluorescence probe, and proton nuclear magnetic resonance study. *J. Biol. Chem.* **1994**, *269*, 28584–28590.
- (21) Nieminen, M. S.; Fruhwald, S.; Heunks, L. M. A.; Suominen, P. K.; Gordon, A. C.; Kivikko, M.; Pollesello, P. Levosimendan: current data, clinical use and future development. *Heart, Lung and Vessels* **2013**, *5*, 227–245.
- (22) Ovaska, M.; Taskinen, J. A model for human cardiac troponin C and for modulation of its Ca²⁺ affinity by drugs. *Proteins: Struct., Funct., Genet.* **1991**, *11*, 79–94.
- (23) Walter, M.; Liebens, I.; Goethals, H.; Renard, M.; Dresse, A.; Bernard, R. Pimobendane (UD-CG 115 BS) in the treatment of severe congestive heart failure. An acute haemodynamic cross-over and double-blind study with two different doses. *Br. J. Clin. Pharmacol.* **1988**, *25*, 323–329.
- (24) Boyle, K. L.; Leech, E. A review of the pharmacology and clinical uses of pimobendan. *Journal of Veterinary Emergency and Critical Care* **2012**, *22*, 398–408.
- (25) Fitton, A.; Brogden, R. N. Pimobendan. A review of its pharmacology and therapeutic potential in congestive heart failure. *Drugs Aging* **1994**, *4*, 417–441.
- (26) Lindert, S.; Li, M. X.; Sykes, B. D.; McCammon, J. A. Computer-Aided Drug Discovery Approach Finds Calcium Sensitizer of Cardiac Troponin. *Chem. Biol. Drug Des.* **2015**, *85*, 99–106.
- (27) Kleerekoper, Q.; Liu, W.; Choi, D.; Putkey, J. A. Identification of Binding Sites for Bepridil and Trifluoperazine on Cardiac Troponin C. *J. Biol. Chem.* **1998**, *273*, 8153–8160.
- (28) Oleszczuk, M.; Robertson, I. M.; Li, M. X.; Sykes, B. D. Solution structure of the regulatory domain of human cardiac troponin C in complex with the switch region of cardiac troponin I and W7: The basis of W7 as an inhibitor of cardiac muscle contraction. *J. Mol. Cell. Cardiol.* **2010**, *48*, 925–933.
- (29) Robertson, I. M.; Sun, Y.-B.; Li, M. X.; Sykes, B. D. A structural and functional perspective into the mechanism of Ca²⁺-sensitizers that target the cardiac troponin complex. *J. Mol. Cell. Cardiol.* **2010**, *49*, 1031–1041.
- (30) Feldkamp, M. D.; O'Donnell, S. E.; Yu, L.; Shea, M. A. Allosteric effects of the antipsychotic drug trifluoperazine on the energetics of calcium binding by calmodulin. *Proteins: Struct., Funct., Genet.* **2010**, *78*, 2265–2282.
- (31) Leelananda, S. P.; Lindert, S. Computational methods in drug discovery. *Beilstein J. Org. Chem.* **2016**, *12*, 2694–2718.
- (32) Genchev, G. Z.; Kobayashi, T.; Lu, H. Calcium induced regulation of skeletal troponin—computational insights from molecular dynamics simulations. *PLoS One* **2013**, *8*, e58313.
- (33) Lindert, S.; Kekenes-Huskey, P. M.; Huber, G.; Pierce, L.; McCammon, J. A. Dynamics and calcium association to the N-terminal regulatory domain of human cardiac troponin C: a multiscale computational study. *J. Phys. Chem. B* **2012**, *116*, 8449–8459.
- (34) Sinko, W.; Lindert, S.; McCammon, J. A. Accounting for Receptor Flexibility and Enhanced Sampling Methods in Computer-Aided Drug Design. *Chem. Biol. Drug Des.* **2013**, *81*, 41–49.
- (35) Amaro, R. E.; Baron, R.; McCammon, J. A. An improved relaxed complex scheme for receptor flexibility in computer-aided drug design. *J. Comput.-Aided Mol. Des.* **2008**, *22*, 693–705.
- (36) Lin, J.-H.; Perryman, A. L.; Schames, J. R.; McCammon, J. A. The relaxed complex method: Accommodating receptor flexibility for drug design with an improved scoring scheme. *Biopolymers* **2003**, *68*, 47–62.
- (37) Lin, J.-H.; Perryman, A. L.; Schames, J. R.; McCammon, J. A. Computational Drug Design Accommodating Receptor Flexibility: The Relaxed Complex Scheme. *J. Am. Chem. Soc.* **2002**, *124*, 5632–5633.
- (38) Barakat, K.; Tuszynski, J. Relaxed complex scheme suggests novel inhibitors for the lyase activity of DNA polymerase beta. *J. Mol. Graphics Modell.* **2011**, *29*, 702–716.
- (39) Barakat, K.; Mane, J.; Friesen, D.; Tuszynski, J. Ensemble-based virtual screening reveals dual-inhibitors for the p53–MDM2/MDMX interactions. *J. Mol. Graphics Modell.* **2010**, *28*, 555–568.
- (40) Barakat, K. H.; Torin Huzil, J.; Luchko, T.; Jordheim, L.; Dumontet, C.; Tuszynski, J. Characterization of an inhibitory dynamic pharmacophore for the ERCC1–XPA interaction using a combined molecular dynamics and virtual screening approach. *J. Mol. Graphics Modell.* **2009**, *28*, 113–130.
- (41) Lindert, S.; Zhu, W.; Liu, Y.-L.; Pang, R.; Oldfield, E.; McCammon, J. A. Farnesyl Diphosphate Synthase Inhibitors from In Silico Screening. *Chem. Biol. Drug Des.* **2013**, *81*, 742–748.
- (42) Lindert, S.; Tallorin, L.; Nguyen, Q. G.; Burkart, M. D.; McCammon, J. A. In silico screening for Plasmodium falciparum enoyl-ACP reductase inhibitors. *J. Comput.-Aided Mol. Des.* **2015**, *29*, 79–87.
- (43) Liu, Y.-L.; Lindert, S.; Zhu, W.; Wang, K.; McCammon, J. A.; Oldfield, E. Taxodione and arenarone inhibit farnesyl diphosphate synthase by binding to the isopentenyl diphosphate site. *Proc. Natl. Acad. Sci. U. S. A.* **2014**, *111*, E2530–E2539.
- (44) Menchon, G.; Bombarde, O.; Trivedi, M.; Négrel, A.; Inard, C.; Giudetti, B.; Baltas, M.; Milon, A.; Modesti, M.; Czaplicki, G.; Calsou, P. Structure-Based Virtual Ligand Screening on the XRCC4/DNA Ligase IV Interface. *Sci. Rep.* **2016**, *6*, 22878.
- (45) Wong, C. F. Conformational transition paths harbor structures useful for aiding drug discovery and understanding enzymatic mechanisms in protein kinases. *Protein Science: A Publication of the Protein Society* **2016**, *25*, 192–203.

- (46) Bhutani, I.; Loharch, S.; Gupta, P.; Madathil, R.; Parkesh, R. Structure, dynamics, and interaction of Mycobacterium tuberculosis (Mtb) DprE1 and DprE2 examined by molecular modeling, simulation, and electrostatic studies. *PLoS One* **2015**, *10*, e0119771–e0119771.
- (47) Lindert, S.; Zhu, W.; Liu, Y.-L.; Pang, R.; Oldfield, E.; McCammon, J. A. Farnesyl Diphosphate Synthase Inhibitors from In Silico Screening. *Chem. Biol. Drug Des.* **2013**, *81*, 742–748.
- (48) Geppert, H.; Vogt, M.; Bajorath, J. Current Trends in Ligand-Based Virtual Screening: Molecular Representations, Data Mining Methods, New Application Areas, and Performance Evaluation. *J. Chem. Inf. Model.* **2010**, *50*, 205–216.
- (49) Lyne, P. D. Structure-based virtual screening: an overview. *Drug Discovery Today* **2002**, *7*, 1047–1055.
- (50) Wang, X.; Li, M. X.; Sykes, B. D. Structure of the Regulatory N-domain of Human Cardiac Troponin C in Complex with Human Cardiac Troponin I147–163 and Bepridil. *J. Biol. Chem.* **2002**, *277*, 31124–31133.
- (51) Li, A. Y.; Lee, J.; Borek, D.; Otwinowski, Z.; Tibbitts, G. F.; Paetzel, M. Crystal Structure of Cardiac Troponin C Regulatory Domain in Complex with Cadmium and Deoxycholic Acid Reveals Novel Conformation. *J. Mol. Biol.* **2011**, *413*, 699–711.
- (52) Hoffman, R. M. B.; Sykes, B. D. Structure of the Inhibitor W7 Bound to the Regulatory Domain of Cardiac Troponin C. *Biochemistry* **2009**, *48*, 5541–5552.
- (53) Durrant, J. D.; de Oliveira, C. A. F.; McCammon, J. A. POVME: An Algorithm for Measuring Binding-Pocket Volumes. *J. Mol. Graphics Modell.* **2011**, *29*, 773–776.
- (54) Sastry, G. M.; Adzhigirey, M.; Day, T.; Annabhimoju, R.; Sherman, W. Protein and ligand preparation: parameters, protocols, and influence on virtual screening enrichments. *J. Comput.-Aided Mol. Des.* **2013**, *27*, 221–234.
- (55) Halgren, T. A.; Murphy, R. B.; Friesner, R. A.; Beard, H. S.; Frye, L. L.; Pollard, W. T.; Banks, J. L. Glide: A New Approach for Rapid, Accurate Docking and Scoring. 2. Enrichment Factors in Database Screening. *J. Med. Chem.* **2004**, *47*, 1750–1759.
- (56) Friesner, R. A.; Banks, J. L.; Murphy, R. B.; Halgren, T. A.; Klicic, J. J.; Mainz, D. T.; Repasky, M. P.; Knoll, E. H.; Shelley, M.; Perry, J. K.; Shaw, D. E.; Francis, P.; Shenkin, P. S. Glide: A New Approach for Rapid, Accurate Docking and Scoring. 1. Method and Assessment of Docking Accuracy. *J. Med. Chem.* **2004**, *47*, 1739–1749.
- (57) Friesner, R. A.; Murphy, R. B.; Repasky, M. P.; Frye, L. L.; Greenwood, J. R.; Halgren, T. A.; Sanschagrin, P. C.; Mainz, D. T. Extra Precision Glide: Docking and Scoring Incorporating a Model of Hydrophobic Enclosure for Protein–Ligand Complexes. *J. Med. Chem.* **2006**, *49*, 6177–6196.
- (58) Banks, J. L.; Beard, H. S.; Cao, Y.; Cho, A. E.; Damm, W.; Farid, R.; Felts, A. K.; Halgren, T. A.; Mainz, D. T.; Maple, J. R.; Murphy, R.; Philipp, D. M.; Repasky, M. P.; Zhang, L. Y.; Berne, B. J.; Friesner, R. A.; Gallicchio, E.; Levy, R. M. Integrated Modeling Program, Applied Chemical Theory (IMPACT). *J. Comput. Chem.* **2005**, *26*, 1752–1780.
- (59) *Maestro*; Schrodinger Release 2016-4; Schrodinger, LLC: New York, 2016.
- (60) *LigPrep*; Schrodinger Release 2016-4; Schrodinger, LLC: New York, 2016.
- (61) Greenwood, J. R.; Calkins, D.; Sullivan, A. P.; Shelley, J. C. Towards the comprehensive, rapid, and accurate prediction of the favorable tautomeric states of drug-like molecules in aqueous solution. *J. Comput.-Aided Mol. Des.* **2010**, *24*, 591–604.
- (62) Shelley, J. C.; Cholleti, A.; Frye, L. L.; Greenwood, J. R.; Timlin, M. R.; Uchimaya, M. Epik: a software program for pKa prediction and protonation state generation for drug-like molecules. *J. Comput.-Aided Mol. Des.* **2007**, *21*, 681–691.
- (63) Harder, E.; Damm, W.; Maple, J.; Wu, C.; Reboul, M.; Xiang, J. Y.; Wang, L.; Lupyan, D.; Dahlgren, M. K.; Knight, J. L.; Kaus, J. W.; Cerutti, D. S.; Krilov, G.; Jorgensen, W. L.; Abel, R.; Friesner, R. A. OPLS3: A Force Field Providing Broad Coverage of Drug-like Small Molecules and Proteins. *J. Chem. Theory Comput.* **2016**, *12*, 281–296.
- (64) Shivakumar, D.; Williams, J.; Wu, Y.; Damm, W.; Shelley, J.; Sherman, W. Prediction of Absolute Solvation Free Energies using Molecular Dynamics Free Energy Perturbation and the OPLS Force Field. *J. Chem. Theory Comput.* **2010**, *6*, 1509–1519.
- (65) Jorgensen, W. L.; Tirado-Rives, J. The OPLS [optimized potentials for liquid simulations] potential functions for proteins, energy minimizations for crystals of cyclic peptides and crambin. *J. Am. Chem. Soc.* **1988**, *110*, 1657–1666.
- (66) Jorgensen, W. L.; Maxwell, D. S.; Tirado-Rives, J. Development and Testing of the OPLS All-Atom Force Field on Conformational Energetics and Properties of Organic Liquids. *J. Am. Chem. Soc.* **1996**, *118*, 11225–11236.
- (67) Triballeau, N.; Acher, F.; Brabet, I.; Pin, J.-P.; Bertrand, H.-O. Virtual Screening Workflow Development Guided by the “Receiver Operating Characteristic” Curve Approach. Application to High-Throughput Docking on Metabotropic Glutamate Receptor Subtype 4. *J. Med. Chem.* **2005**, *48*, 2534–2547.
- (68) Hawkins, P. C. D.; Kelley, B. P.; Warren, G. L. The Application of Statistical Methods to Cognate Docking: A Path Forward? *J. Chem. Inf. Model.* **2014**, *54*, 1339–1355.
- (69) Davis, J. P.; Norman, C.; Kobayashi, T.; Solaro, R. J.; Swartz, D. R.; Tikunova, S. B. Effects of thin and thick filament proteins on calcium binding and exchange with cardiac troponin C. *Biophys. J.* **2007**, *92*, 3195–3206.
- (70) Siddiqui, J. K.; Tikunova, S. B.; Walton, S. D.; Liu, B.; Meyer, M.; de Tombe, P. P.; Neilson, N.; Kekenes-Huskey, P. M.; Salhi, H. E.; Janssen, P. M. L.; Biesiadecki, B. J.; Davis, J. P. Myofilament Calcium Sensitivity: Consequences of the Effective Concentration of Troponin I. *Front. Physiol.* **2016**, *7*, 7.
- (71) Robertson, S.; Potter, J. D. The regulation of free Ca²⁺ ion concentration by metal chelators. *Methods in Pharmacology* **1984**, *5*, 63–75.
- (72) Feixas, F.; Lindert, S.; Sinko, W.; McCammon, J. A. Exploring the role of receptor flexibility in structure-based drug discovery. *Biophys. Chem.* **2014**, *186*, 31–45.
- (73) Sinko, W.; de Oliveira, C.; Williams, S.; Van Wynsberghe, A.; Durrant, J. D.; Cao, R.; Oldfield, E.; McCammon, J. A. Applying Molecular Dynamics Simulations to Identify Rarely Sampled Ligand-bound Conformational States of Undecaprenyl Pyrophosphate Synthase, an Antibacterial Target. *Chem. Biol. Drug Des.* **2011**, *77*, 412–420.
- (74) Solaro, R. J.; Bousquet, P.; Johnson, J. D. Stimulation of cardiac myofilament force, ATPase activity and troponin C Ca⁺⁺ binding by bepridil. *Journal of Pharmacology and Experimental Therapeutics* **1986**, *238*, 502–507.
- (75) Williams, M.; Malick, J. B. *Drug Discovery and Development*; Springer Science & Business Media, Clifton, NJ, 2012; p 453.
- (76) Baell, J. B.; Holloway, G. A. New Substructure Filters for Removal of Pan Assay Interference Compounds (PAINS) from Screening Libraries and for Their Exclusion in Bioassays. *J. Med. Chem.* **2010**, *53*, 2719–2740.
- (77) Dahlin, J. L.; Nissink, J. W. M.; Strasser, J. M.; Francis, S.; Higgins, L.; Zhou, H.; Zhang, Z.; Walters, M. A. PAINS in the Assay: Chemical Mechanisms of Assay Interference and Promiscuous Enzymatic Inhibition Observed during a Sulfhydryl-Scavenging HTS. *J. Med. Chem.* **2015**, *58*, 2091–2113.
- (78) Alland, C.; Moreews, F.; Boens, D.; Carpentier, M.; Chiusa, S.; Lonquety, M.; Renault, N.; Wong, Y.; Cantalloube, H.; Chomilier, J.; Hochez, J.; Pothier, J.; Villoutreix, B. O.; Zagury, J. F.; Tufféry, P. RPBS: a web resource for structural bioinformatics. *Nucleic Acids Res.* **2005**, *33*, W44–W49.
- (79) Neron, B.; Ménager, H.; Maufrais, C.; Joly, N.; Maupetit, J.; Letort, S.; Carrere, S.; Tuffery, P.; Letondal, C. Mobylye: a new full web bioinformatics framework. *Bioinformatics* **2009**, *25*, 3005–3011.
- (80) Lagorce, D.; Sperandio, O.; Baell, J. B.; Miteva, M. A.; Villoutreix, B. O. FAF-Drugs3: a web server for compound property calculation and chemical library design. *Nucleic Acids Res.* **2015**, *43*, W200–W207.

(81) Stepan, A. F.; Walker, D. P.; Bauman, J.; Price, D. A.; Baillie, T. A.; Kalgutkar, A. S.; Aleo, M. D. Structural Alert/Reactive Metabolite Concept as Applied in Medicinal Chemistry to Mitigate the Risk of Idiosyncratic Drug Toxicity: A Perspective Based on the Critical Examination of Trends in the Top 200 Drugs Marketed in the United States. *Chem. Res. Toxicol.* **2011**, *24*, 1345–1410.

(82) Abou-Gharbia, M. Discovery of Innovative Small Molecule Therapeutics. *J. Med. Chem.* **2009**, *52*, 2–9.

(83) Aldrich, C.; Bertozzi, C.; Georg, G. I.; Kiessling, L.; Lindsley, C.; Liotta, D.; Merz, K. M.; Schepartz, A.; Wang, S. The Ecstasy and Agony of Assay Interference Compounds. *ACS Cent. Sci.* **2017**, *3*, 143–147.

(84) Vasquez-Martinez, Y.; Ohri, R. V.; Kenyon, V.; Holman, T. R.; Sepúlveda-Boza, S. Structure–activity relationship studies of flavonoids as potent inhibitors of human platelet 12-hLO, reticulocyte 15-hLO-1, and prostate epithelial 15-hLO-2. *Bioorg. Med. Chem.* **2007**, *15*, 7408–7425.

(85) Cathcart, M. K.; Folcik, V. A. Lipoxygenases and atherosclerosis: protection versus pathogenesis. *Free Radical Biol. Med.* **2000**, *28*, 1726–1734.

(86) Neuzil, J.; Upston, J. M.; Witting, P. K.; Scott, K. F.; Stocker, R. Secretory Phospholipase A2 and Lipoprotein Lipase Enhance 15-Lipoxygenase-Induced Enzymic and Nonenzymic Lipid Peroxidation in Low-Density Lipoproteins[†]. *Biochemistry* **1998**, *37*, 9203–9210.

(87) Kayama, Y.; Minamino, T.; Toko, H.; Sakamoto, M.; Shimizu, I.; Takahashi, H.; Okada, S.; Tateno, K.; Moriya, J.; Yokoyama, M.; Nojima, A.; Yoshimura, M.; Egashira, K.; Aburatani, H.; Komuro, I. Cardiac 12/15 lipoxygenase–induced inflammation is involved in heart failure. *J. Exp. Med.* **2009**, *206*, 1565–1574.

(88) Backman, T. W. H.; Cao, Y.; Girke, T. ChemMine tools: an online service for analyzing and clustering small molecules. *Nucleic Acids Res.* **2011**, *39*, W486–W491.

(89) Takeda, S.; Yamashita, A.; Maeda, K.; Maeda, Y. Structure of the core domain of human cardiac troponin in the Ca²⁺-saturated form. *Nature* **2003**, *424*, 35–41.

(90) Ohio Supercomputer Center, 1987. <http://osc.edu/ark:/19495/f5s1ph73> (accessed November 2017).